

Soil Shear Strength Assessment for erosion hazards prevention

Kempena Adolphe¹, MouandaMakandaEmilienne Grève², Rafael Guardado Lacaba³, Antonio Olimpio Gonçalves⁴, MbilouUrbainGampio⁵, Boudzoumou Florent⁶.

¹(Departement of Geology, Faculty of Sciences and Technics, MarienNgouabi University, Brazzaville-Congo)

²(Departement of Geology, Faculty of Sciences and Technics, MarienNgouabi University, Brazzaville-Congo)

³(Departement of Geology, Faculty of Mines and Geology, Higher Institute of Mines and Metallurgy, Moa-CUBA)

⁴(Departement of Geology, Faculty of Sciences, Agostinho Neto University, Luanda-Angola)

⁵(Departement of Geology, Faculty of Sciences and Technics, MarienNgouabi University, Brazzaville-Congo)

⁶(Departement of Geology, Faculty of Sciences and Technics, MarienNgouabi University, Brazzaville-Congo)

Abstract:

Soil improvement using the geosynthetic layer technique is usually used for resolving many geotechnical problems. This technique provides a reinforced soil with high shear strength against erosion phenomenon that destroy foundations and lead to losses of human lives in Brazzaville City. The interest is certainly well displayed. Indeed, this work aims to experimentally assess the geosynthetics placement influence on the fine sand properties against water erosion phenomenon. An experimental program has been carried for fine sand to study the soil shear strength from the soil not/and reinforced by geosynthetic layers. This made it possible to assess the soil displacements during the direct shear test. This opens the door to understand the geosynthetics effect in the soil for enhancing the soil shear strength for its possible use as a prevention method against soil erosion.

Key words: Shear strength; geosynthetics; erosion; reinforcement; reinforced soil.

Date of Submission: 20-06-2022

Date of Acceptance: 03-07-2022

I. Introduction

Various historical cases demonstrate that fine sands are sensitive to erosion risk and its improvement by using geosynthetics can reinforce the soil strength against water erosion phenomenon. This erosion phenomenon related to the reinforced soil strength has the effects on the erosion resistance on fine sands deposits [1, 2, 3, 4, 5]. There is argument on the reasons of reduction in the erosion resistance at smaller or similar soil strength [4, 5] performed tests to five sands with difference in gradation characteristics ($D_{10}=0.11-0.40\text{mm}$, $C_u=1.53-2.57$) in order to evaluate the gradational characteristics role of soil on the erosion resistance. They used the soil strength as input parameters for erosion resistance analysis. Then they concluded that erosion and soil reinforcement resistances correlate well with a single index property such as cohesion. Though, compressibility associated with the grain size of the reinforced fine sand shows the reasonable correlation with erosion resistance.

To this end, soil reinforcement contributes to modify soil properties by physical action or by inclusion of a more resistant material in the soil. In addition to this, it is noted that soils stability in geotechnical projects is an essential condition and their properties can be improved by reinforcement techniques. This is why the design of earthen structures using geosynthetics has made it possible to understand the beneficial effects of soil plane reinforcement. The soils constitutive law being particularly complex, a soil rupture does not pose only a problem of rupture kinematics choice. It is also necessary to define when the rupture occurs in the tests which serve for soil shear strength measurement. Such as direct shear tests which allow the soil strength parameters measurement, either the angle of friction (ϕ') or the cohesion (c') and the angle of dilatancy (ψ) [6].

The aim of this work is to assess the soil shear strength under reinforced conditions or not. This is important for economic development and demographic expansion of Brazzaville city which has led to its agglomerations extension which is now pushing us to settle ourselves in practically all sites and on all types of soil, even those with poor mechanical and physical properties deemed unbuildable [7].

Study area

Brazzaville city is located on the right bank of the Congo River downstream of the Stanley Pool. It is located in cartographic zone 33S and has a latitude between $4^{\circ} 11'45''$ and $4^{\circ} 18'45''$ South and a longitude between $15^{\circ} 11'15''$ and $15^{\circ} 18'45''$ East (Figure 1). The study area has a climate of the Lower Congolese or Sudano Guinean type, characterized by two seasons as a long rainy season from October to May, interrupted by a small dry season from January to February and a long dry season from June to September [8]. It is found a contrasting landscape juxtaposing the reliefs of plateaus and plains [9]. The groundwater in the region is a veritable Congo water tower from which the rivers of Congo and Gabon were originated [10]. The soils are varied and we can distinguish soils formed on polymorphic Batéké sands with a clay content and very low mineral reserves, soils formed on Inkisi sandstone with a sandy-clay texture, soils formed on heterogeneous alluvial deposits of the Congo River and its tributaries. These soils are generally sandy clay poor in organic matter [11, 12]. Geological formations encountered in the region are divided into three large sedimentary series which from the base to the top appear respectively the Inkisi Formation, the Stanley-Pool Series and the Batéké Plateaus Series [13, 14, 15].

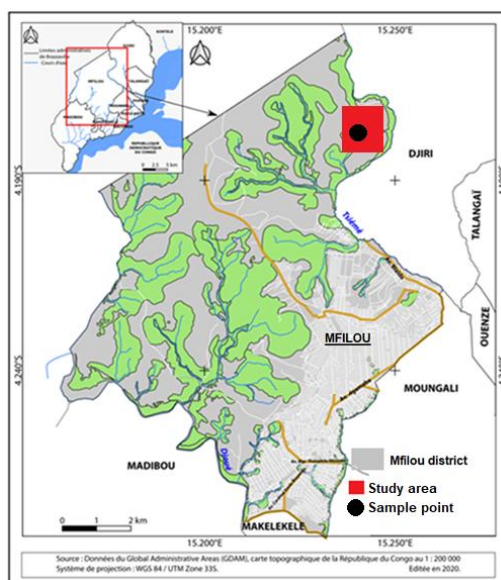


Figure 1. Study area location

II. Material and Methods

Materials used and experimental study

It was used for this study a soil sample in a 30 kg pocket at a depth of approximately 0.75 m, precisely at the foot of the slope in the Djiri-Magnanga district located at the northern zone of Brazzaville City (Figure 1).

Laboratory tests

1. Grains size analysis
2. Specific densities of solid grains
3. Atterberg limits
4. Modified Proctor test
5. Shear test

The laboratory equipment used belongs to the Road Geotechnical Laboratory.

Grains size analysis

The soil studied is sand taken from a bag of 30 kg. It is done by dry sieving after washing for soils with solid particles size greater than $80\ \mu\text{m}$ and by sedimentation for soil elements with size less than $80\ \mu\text{m}$. Soil grain size analysis up to a diameter of $80\ \mu\text{m}$ is done using a series of sieves.

Grains size test by sieving

The test objective is to determine the mass of grains by diameter up to $80\ \mu\text{m}$ there are two methods:

1. Wet sieving.
2. Dry sieving after washing (NFP94-056 / 1996)

Equipment

1. Sieve in general, square mesh screens
2. Common dimensions: 80 mm - 50 mm - 32 mm - 20 mm - 10 mm - 5 mm - 2 mm - 1 mm - 0.4 mm - 0.2 mm - 0.08 mm (= 80µm)
3. Balance.

Grains size test by sedimentometry

The aim of sedimentometry is to determine the grains weight distribution of soil according to their size for fine particles smaller than 0.08 mm. Indeed, when the grains diameter is small, sieving no longer makes it possible to obtain accurate results (NFP94-057 / 1992).

Mechanical tests

In order to obtain a better knowledge of the soil mechanical behavior before and after the reinforcement, the following mechanical tests were carried out:

Modified Proctor test

The Modified Proctor test is carried out according to the standard [NF P 94-093]. The purpose of the Proctor test is to determine the optimum water content and the maximum density of a material subjected to standardized compaction of a given intensity.

Direct shear test

Test on unreinforced samples: The goal is to put the shear plane in the middle of a layer, so vertically the sample is considered homogeneous.

Equipment: The specific device under test comprises (see Figure 10).

1. The shear box with internal section $A = 100 \text{ cm}^2$ and a height of 1.9 cm composed of two half-boxes.
2. The device for applying the desired normal force and the device producing the relative horizontal displacement between the two half-boxes,
3. A dynamometric ring indicating the shear forces,
4. The force sensors: The horizontal sensor of the digital ruler type, records the movements of the upper box and allows the speed regulation of this box; the vertical sensor, also with a digital ruler type, measures the settlement or general materials dilatancy during the test.

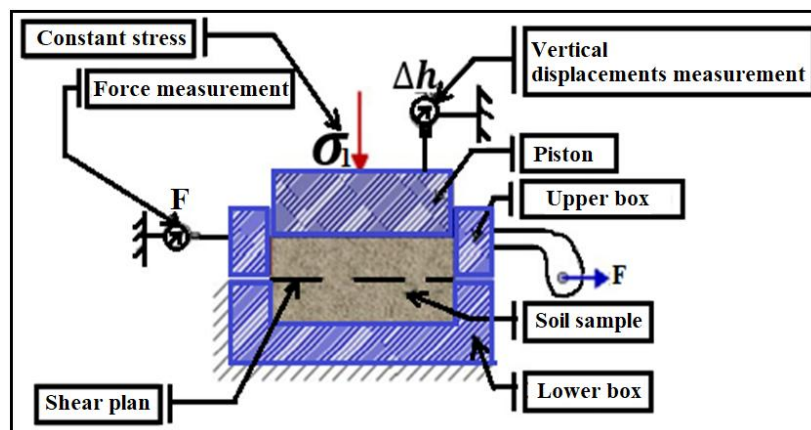


Figure 2. Schematic of the shear box

Reinforced samples test

The reinforcement layer is positioned in the middle of the sample height between the fixed lower box and the movable upper box of the test device.

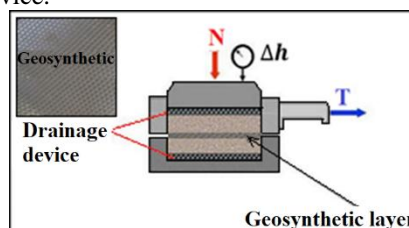


Figure 3. Geosynthetic layer position in the sample during the test

III. Result

Grains size test

A total of three grains size tests were carried out on the homogeneous sand and are shown in Figure 4.

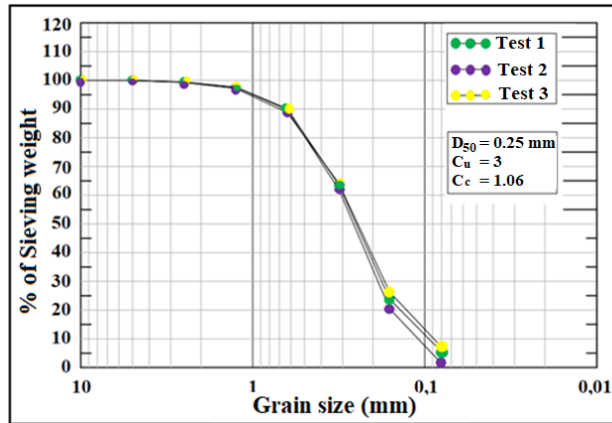


Figure 4. Grains size curve

The average diameter (D_{50}) is 0.25 mm and the sand does not contain any particles larger than 5 mm. The coefficient of uniformity (C_u) and the coefficient of curvature (C_c) are 3 and 1.06 respectively. The fine particles percentage is 7% on average. Thus according to the grain size distribution analysis and the USCS classification (ASTM D2487) the soil is considered as a fine uniform sand with little silt (SP).

Modified Proctor Test

The curve of which the Modified Proctor test is shown in Figure 18 which establishes the relationship between the material water content (w) and the dry density (γ_d). This test establishes the optimum water content which is useful to promote the placement of sand in the test cell. If the sample water content is varied and the variation of γ_d is graphically represented as a function of water content (w). It is obtained a bell curve which presents a high point called Proctor optimum (Figure 5).

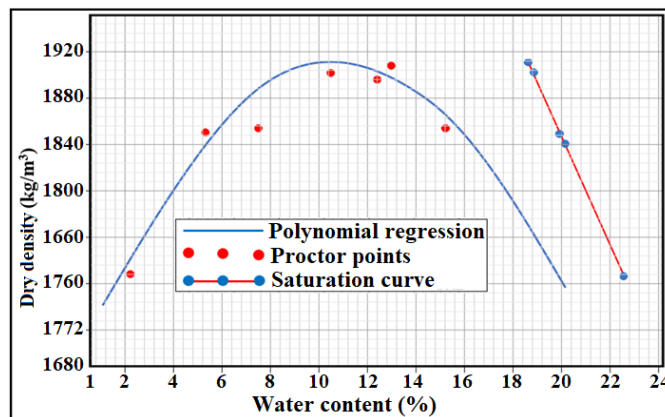


Figure 5. Modified Proctor Curve

This phenomenon is easily explained when the water content is high, water absorbs a large part of the compaction energy without any profit, moreover it takes the place of solid grains; on the other hand when the water content is low, water has a significant lubricating role and the dry density increases with the water content. On the curve left side called the dry side, the voids volume is occupied by water and air. On the right side called the wet side, water occupies practically all the voids. The optimum water content is around 10.7% and the saturation water content is around 20%.

Table no 1: Laboratory tests results

Parameters	Symbol	Value	Standard deviation	Unit
Specific density	G_s	2,73	0,00	---
Optimal water content	ω_{opt}	10,7	0,00	%
Maximum density	ρ_{max}	1860	10,7	kg/m ³

Minimum density	ρ_{min}	1560	20,6	kg/m ³
Internal friction angle (large deformation)	ϕ_{gd}	34,3	---	°
Angle of internal friction at peaks (dense soil)	ϕ_{pic}	43,2	---	°
Angle of dilatancy	ψ	5,7	1,42	°
Sand portion	---	93	---	%
Silt portion	---	7	---	%
Plasticity Index	IP	5.0
Cohesion	c	1,7	kPa

Direct shear tests

Direct shear tests allow the soil strength parameters measurement namely the friction angle (ϕ') and the angle of dilatancy (ψ). The friction angle is obtained according to the tangent arc of the shear stress ratio (τ) at large strain on the vertical stress (σ_v) and the angle of dilatancy by the vertical displacement ratio (U_y) to the horizontal displacement (U_x) in the dilatation zone. A total of 6 tests are performed, 3 under expanding conditions and 3 under contracting conditions under vertical stresses of 50, 150 and 400 kPa. Figure 6 shows the τ/U_x plane and Figure 7 shows the U_y/U_x plane and the Figure 8 shows the Mohr-Coulomb framework obtained during these tests.

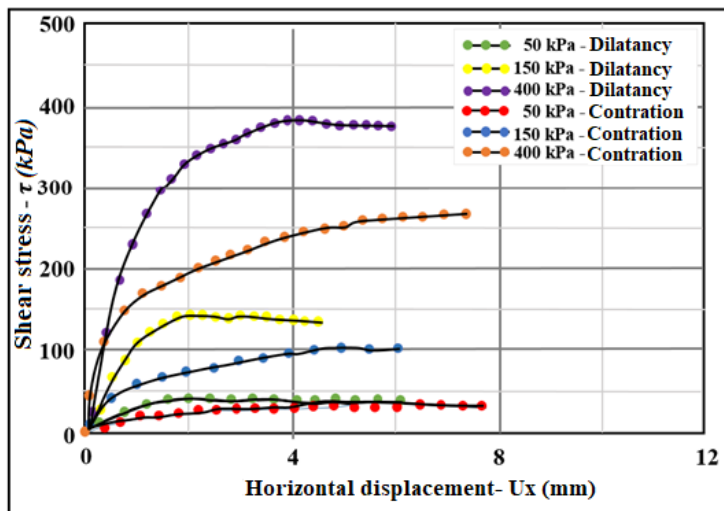


Figure 6. Direct shear test

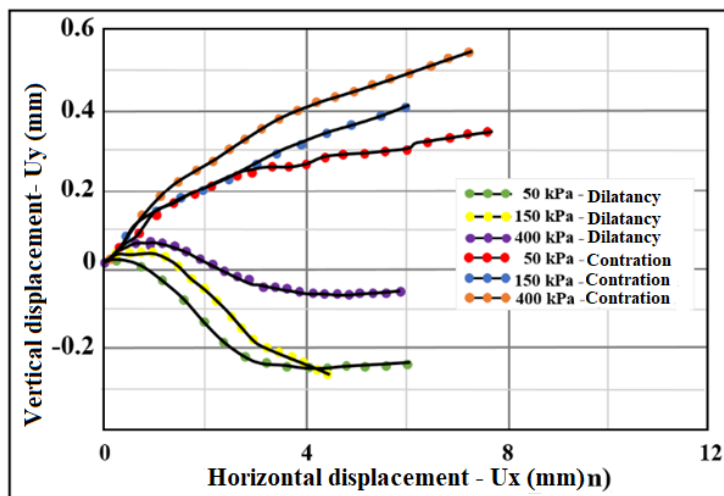


Figure 7. Direct shear test

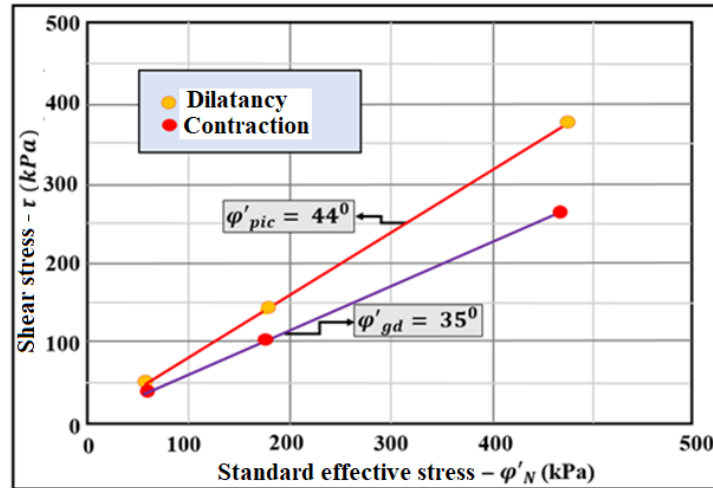


Figure 8. Mohr-Coulomb framework

The direct box shear tests are shown in the following curves:

1. Stresses - strains $\tau = f(\Delta L)$;
2. Intrinsic lines $\tau = f(\sigma)$.

As a function of the applied normal stress (50, 150, 400 KPa); it is shown in the Figure 9 (Curves $\tau = f(\Delta L)$)

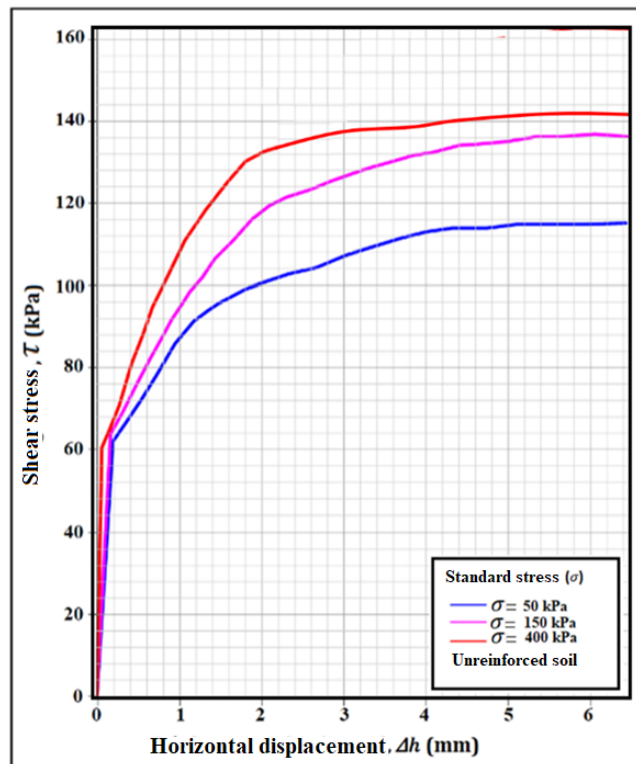


Figure 9. Stress-Strain Curve under compressive Stresses

Figure 9 shows the drained shear strength evolution as a function of the horizontal displacement for tests carried out. It should be noted in Figure 9 that the soil strength characterized by tangential stress increases significantly with the normal or standard stress increase. Peak tangential stress (τ) values of 132, 118 and 100 kPa were obtained for normal or standard stresses $\sigma = 50$, $\sigma = 150$ and $\sigma = 400$ kPa, respectively.

Test on reinforced samples

Placement of geosynthetic layer in the ground: Figure 10 shows the reinforcement layer positioned in the middle of the height of the sample between the fixed lower box and the movable upper box of the testing device.

- a) Curves $\tau = f(\Delta L)$

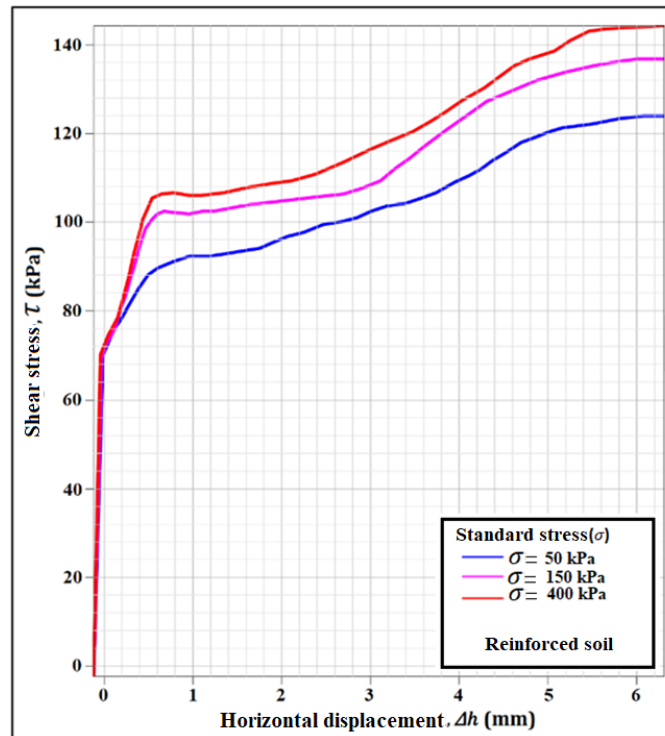


Figure 10. Stress-Strain Curve under compressive Stresses

Figure 10 shows the drained shear strength evolution as a function of the horizontal displacement. Figure 10 that the soil strength characterized by the tangential stress, increases significantly with the increase of the normal or standard stress. Peak tangential stress (τ) values of 150, 125 and 122 kPa were obtained for $\sigma' = 50$, $\sigma' = 150$ and $\sigma' = 400$ kPa, respectively. It is noted that there is a significant improvement in the reinforced soil shear strength. The tangential stress value at the peak of reinforced samples is significantly higher than that of the unreinforced samples. Figure 10 shows that the soil strength characterized by the tangential stress increases significantly with the increase of normal stress in the unreinforced soil. While in the case of reinforced soil it is noted that there is a significant improvement in the reinforced soil shear strength whose shear stress value at the peak is significantly higher than that of unreinforced soil.

According to these observations, the influence of the synthetics to erosion and reinforced soil resistance to erosion can determine at different loading conditions. As shown in Figure 10, the soil strength against erosion phenomena increased as reinforcement technique is used. The increase in the fine sand soil resistance against erosion process depends on the following factors: construction of the new bondsin soil structure during the reinforcement procedure in the soil increasing its relative density, significant densification results in a reinforcement process, (3) increase in soil compression with reinforcement which does not allow sand grains separation by the water action.

IV. Discussion

Geotechnical laboratory tests have made it possible to assess the soil stress-deformation behavior in the face of failure under reinforced or unreinforced conditions. The results of table 2 show that our soil is not very plastic and very deformable. For preventing structures against unexpected erosion destruction, and also for a better understanding of soil mechanics in the laboratory to get a good idea we compared two soil samples, one natural and the other reinforced by geosynthetic layers and the results demonstrated that the value of the shear stress at the peak for reinforced samples is significantly higher than that the unreinforced samples, showing its capability to resist against erosion phenomenon and secure the built areas. Several criteria have been verified in our work as confirmed [16, 17]. The slope of the failure lines increases proportionally with the presence of reinforcement. The more the sample is reinforced the critical rupture stress decreases preventing the soil from rupture and allow its adequate protection against erosion processes. It is noted that for a vertical stress of 400 Kpa, the shear stress is at the maximum and this result can be explained by the rupture traction which increases up to a certain level of stress after which the same decreases.

V. Conclusion

This work was devoted to the characterization and experimental identification of two types of soil, namely natural soil and soil reinforced by geosynthetic layers. It falls within the framework of improving and securing land in urban extensions against erosion hazards. The initial objective of this research work is to study the behavior of soils reinforced by geosynthetic layers and more particularly interaction between soil and geosynthetic reinforcement and the reinforcement influence on the soil erosion prevention. In this work the experimental tests of silty sand reinforced by geosynthetic layers were carried out. Conclusions relating to the experimental and numerical developments carried out were drawn and summarized in the study for identification parameters, in order to better present the physical aspects of the studied materials and to make a general classification of soil and identification tests confirm the presence of silty sand in our study area. For soil samples reinforced with geosynthetic layers and under direct shear tests, taking into account the data and results obtained in this study, we found a significant improvement in the shear strength of the reinforced soil which can contribute to increase the soil resistance against the erosion hazards.

References

- [1]. Mesri, G., Feng, T.W., Benak, J.M. (1990). Post densification penetration resistance of clean sands. *Journal of Geotechnical Engineering*. 116(GT7):1095–1115
- [2]. Ohara, S., Yamamoto, T., Yurino, H. (1992). Experimental study on re-liquefaction potential of saturated and deposit. Paper presented at the tenth world earthquake engineering conference, Balkema, Rotterdam.
- [3]. Oda, M., Kawamoto, K., Fujimori, H., Sato, M. (2001). Microstructural interpretation on re-liquefaction of saturated granular soils under cyclic loading. *Journal of Geotechnical and Geoenvironmental Engineering*. 127(5):416-423.
- [4]. Olson, S.M., Green, R.A., Obermeier, S.F. (2005). Geotechnical analysis of paleoseismic shaking using liquefaction effects: a major updating. *Engineering Geology*. 76:235-61.
- [5]. Ha, I.S., Olson, S.M., Seo, M.W., Kim, M.M. (2011). Evaluation of re-liquefaction resistance using shaking table tests. *Soil Dynamics and Earthquake Engineering*. 31:682-691.
- [6]. Moraci, N. R. (2006). factors affecting the interface apparent coefficient of friction mobilised in pullout conditions. EuroGeo3. Munich, Germany.
- [7]. Kempena, A. (2017). Evaluation des risques d'érosion hydrique dans la ville de Brazzaville. Thèse de doctorat (PhD). Institut Supérieur des Mines et Métallurgie de Moa, Cuba. 100 Pp.
- [8]. Samba-Kimbata, M (1978). The Bas Congo climate. Ph.D. dissertation. C.R.C of Dijon: Burgundy University, 280, 120-133.
- [9]. Moukolo, N (1992). State of current knowledge on the hydrogeology of Congo Brazzaville. *Hydrogeology*. Brazzaville, n°1-2, 47-58.
- [10]. Denis, B (1974). Explanatory note of the Brazzaville-Kinkala soils map. Republic of the Congo. Paris: ORSTOM. 101, p. 27-35.
- [11]. Schwartz, D (1987). Soils around Brazzaville and their use. ORSTOM, Pointe Noire, 50, p.15-17.
- [12]. Cosson, J (1955). Explanatory note about Pointe-Noire and Brazzaville. Geological acknowledgement map at 1/500,000. Brazzaville: Department of Mines and Geology. A.E.F.
- [13]. Marshal, A (1966). Contribution to Bateke's plateau study (Geology, geomorphology, hydrogeology). Brazzaville: ORSTOM. 78, p. 30-35.
- [14]. Dadet, P. (1969). Explanatory note of Geological map of Republic of Congo Brazzaville at 1/500 000. Paris: Reports of BRGM, N°70. 103, p. 108-132.
- [15]. Boudzoumou, F (1986). The West-Congolese chain and its foreland in the Congo: relations with the Mayombian. Sedimentation of Upper Proterozoic sequences. Ph.D. dissertation. University of Law, Economics and Sciences of Aix-Marseille, Republic French. 220, p. 101-133.
- [16]. SERE, A. (2010). Ouvrages renforcés par géotextiles chargés en tête: comportement et dimensionnement. Paris: HAL.
- [17]. Reiffsteck, P. (1996). Etude du comportement mécanique du géotextile tridimensionnel alvéolaire ARMATER-Analyse numérique et expérimentale. Thèse de doctorat, Université Blaise Pascal Clermont II.

Kempena Adolphe, et. al. Soil Shear Strength Assessment for erosion hazards prevention." *IOSR Journal of Environmental Science, Toxicology and Food Technology (IOSR-JESTFT)*, 16(7), (2022): pp 01-08.